ELSEVIER

Chemical Engineering Journal 135S (2008) S110–S116

Chemical Engineering Journal

www.elsevier.com/locate/cej

Reactive particle precipitation in liquid microchannel flow

N. Kockmann *, J. Kastner, P. Woias

Laboratory for Design of Microsystems, Department of Microsystems Engineering (IMTEK), Albert-Ludwig University of Freiburg, Georges Koehler-Allee 102, D-79110 Freiburg, Germany

Abstract

Continuous precipitation by mixing of two fluids is a simple and important method to produce nanoparticles for many industrial applications in specialty chemistry, pharmacy, or food industry. The convective mixing and mass transfer determine the nucleation and growth of the nanoparticles, resulting in the final particle size distribution. We have studied the ability of T-shaped silicon micromixers for reactive precipitation of nanoparticles. The mixer chips have a straight mixing channel to minimize particle attachment and blocking. The experimental results show a narrow particle size distribution for the precipitation of barium sulfate ($BaSO_4$) over a wide operation range. The particle nucleation is modelled with the classical thermodynamic nucleation theory. The growth of a single particle is analytically described by the diffusive mass transfer in its vicinity and the Sherwood number, while particle interactions are neglected. The T-shaped micromixers are also used to investigate azo coupling under industrial conditions. With these results, basic rules for design and operation of the mixing device are given to prevent clogging and reduce fouling.

Keywords: Microreactor; Barium sulfate; Nucleation; Particle size distribution; Azo coupling

1. Introduction

Particle processes are widely spread in chemical engineering with many applications in specialty and fine chemistry, pharmaceutical and food technology. Particle processing in microchannels has its difficulties due to wall attachment of particles and following fouling and blocking of the passages. On the other hand the transfer processes, the mixing of reactants as well as the residence time are very fast in microstructured devices [1] which is favorable for the generation of nanosized particles with a narrow size distribution. Particle-generating processes have been realized in micromixing devices mostly for scientific purposes, e.g. $BaSO_4$ precipitation, but also for industrial applications like pigment synthesis. Nevertheless, there is some recent work investigating the behavior and advantages of microstructure devices for fabrication of (nano-)particles. Besides the thorough studies of Schwarzer et al. [2–5] on the precipitation of $BaSO_4$ within T-shaped micromixers, there are only few publications dealing with particle generation in microchannels [6–8]. Of particular interest are reports about the production and conditioning of dye pigments in microreactors: Pennemann et al. [9] describe the synthesis of the azo pigment Yellow 12 in a microreactor and the accompanying improvement of its properties. Clariant, a manufacturer of fine chemicals, has patented the production and conditioning, i.e. the improvement of the pigment properties by physical treatment of diketopyrrolopyrrol pigments in a microreactor [10,11].

Passive micromixers are based on two main principles, i.e. multilamination and convective mixing. In multilamination two or more fluids are shaped into stacks of alternating phases, so-called lamellae. A good review on this class of micromixers is given in Hessel et al. [12]. During convective mixing, the fluids are mixed by viscous-convective mixing, in which lamellae of alternating composition are formed. Although the flow regime is also laminar, the fluid elements are continuously stretched and thinned due to convective fluid motion induced by flow redirections. One of the simplest types of this class is the T-shaped micromixer, which exhibits the characteristic engulfment flow [13,14]. Transient flow regimes appear in the T-shaped micromixer at Reynolds numbers, *Re*, in the mixing channel of about 250–300. The entire flow regimes in symmetric mixing in T-shaped micromixers are described by Kockmann et al. [15] with the appearance of flow and pressure pulsations at *Re* numbers larger than 400.

This paper investigates the basic relations between convective mixing in T-shaped micromixers and their influence on particle precipitation. For this purpose a model for coupled mixing-precipitation processes is derived and numerically simulated.

* Corresponding author. Tel.: +49 761 203 7499; fax: +49 761 203 7492.
E-mail address: kockmann@imtek.de (N. Kockmann).

1385-8947/$ – see front matter © 2007 Elsevier B.V. All rights reserved.
doi:10.1016/j.cej.2007.07.042

The results are compared to experimental data gained from the precipitation of $BaSO_4$, a widely used model system for reactive precipitation [2]. Further, the suitability of convective micromixing devices for industrial pigment synthesis is evaluated in collaboration with Ciba Specialty Chemicals Inc. (Ciba). Both objectives demand for micromixers with special properties. Hence, design rules have to be established for basic mixing devices, which are subsequently implemented and realized by the aid of silicon bulk micromachining.

2. Modeling and simulation

Considering a single particle, precipitation can be divided into three distinct stages: nucleation, growth, and secondary effects (e.g. aggregation). Nucleation and growth only occur if the solute concentration (or activity) exceeds the solubility K_{sp}. The solute concentration relative to the solubility is measured with the saturation ratio S. For $S>1$ the solution is called supersaturated and enables nucleation and particle growth. For precipitation of barium sulfate from sulfuric acid and barium chloride solution according to the net formula

$$H_2SO_4 + BaCl_2 \rightarrow BaSO_4\downarrow + 2HCl, \quad (1)$$

the saturation ratio calculates to

$$S = \gamma\sqrt{\frac{c(Ba^{2+})c(SO_4{}^{2-})}{K_{sp}}}. \quad (2)$$

In this study, the mean activity coefficient γ is estimated with the Bromley method, and, for computation of the effective ion concentrations $c(Ba^{2+})$ and $c(SO_4{}^{2-})$, the incomplete dissociation of sulfuric acid has to be considered, as well as complex formation between Ba^{2+} and $SO_4{}^{2-}$ [4,16].

If barium chloride is added in excess, aggregation is slow due to electrostatic stabilization of the formed particles by adsorption of barium ions [4]. Thus we can ignore secondary effects if we only want to compute the particle size distribution immediately after completion of precipitation.

Since the precipitation process within convective micromixers includes length scales from nm range for particle nucleation, up to some 100 μm for convective mixing, the coupled direct numerical simulation of thermodynamics and 3D flow is too complex and time-consuming. Instead, a reduced-order model for precipitation of barium sulfate in T-shaped micromixers is applied: while nucleation and particle growth are implemented by the classical theories of homogeneous nucleation and diffusion, the mixing process is taken into account only by calculating the mean thermodynamic properties within the reaction zone due to diffusion and convective stretching of a virtual fluid lamella with mean thickness.

2.1. Nucleation and diffusion-controlled growth

Although the condition $S>1$ is necessary for solid formation, it is not sufficient for nucleation. The formation of a new phase requires additional energy, which, by classical theory, attributes to the surface tension σ between solid and liquid phase [17]. For a cluster of N molecules, this surface energy is $\sim N^{2/3}$; the energy released due to the phase transition on the other hand is $\sim N$. Hence, there is a critical size N^* for which both energy quantities are equal. The corresponding cluster of molecules is called the critical nucleus, and only particles having reached this size can grow further. Nucleation is called homogeneous if the nucleus only consist of the precipitating species, and heterogeneous if impurities or fragments of larger crystals serve as critical nucleus.

For high supersaturations S as encountered in this study, homogeneous nucleation is the predominant mechanism and the rate of nucleation B can be computed in terms of supersaturation and surface tension σ [17]. However, various models exist for the nucleation rate of barium sulfate; the approach used in this study is presented by Schwarzer [2].

After formation of the critical nucleus, the particle grows continuously as long as the ambient fluid is supersaturated. According to Mersmann et al. [18], particle growth is controlled by the transport of the precipitating species to the particle surface for $S>40$. For spherical particles with diameter L, the linear growth rate $G = dL/dt$ can be expressed in terms of the diffusivity D (here $D = 1.67 \times 10^{-9}\ m^2/s$), the molar density of the solid c_s, the dimensionless Sherwood number Sh for mass transfer around a particle, and the growth potential ψ:

$$G = \frac{2DSh}{Lc_s}\psi \quad (3)$$

For precipitation of a single component the growth potential is just the difference between the concentration in the bulk fluid and near the particle surface. In the binary system of barium sulfate, the effective concentration $\gamma\sqrt{c(Ba^{2+})c(SO_4{}^{2-})}$ has to be used instead [18], thus:

$$\psi = \sqrt{K_{sp}}(S-1). \quad (4)$$

A detailed discussion of transport-controlled particle growth can be found in Söhnel and Garside [17].

2.2. Particle size distribution and population balance

The primary goal of precipitation modeling is to predict the particle size distribution (PSD), given the initial concentrations and mixing conditions. The PSD is the relative frequency $\tilde{n}$ of particles with size between L and $L+dL$, assuming spherical shape. Since precipitated particles normally exhibit some type of crystal structure, L actually is the equivalent size of a sphere with the same volume.

The key to PSD simulations is the population balance equation, which relates the concentration $n(L)$ of particles with size L to particle growth G and nucleation b per unit volume [19]:

$$\frac{\partial n}{\partial t} + \frac{\partial(Gn)}{\partial L} = b. \quad (5)$$

Since we do not consider secondary effects, the terms for aggregation and particle death are omitted from the complete population balance. Both, G and b depend on the local concentrations of the precipitating species. Except for the case of

instantaneous ideal mixing, the PSD simulation consequently requires combining Eq. (5) with a mixing model. The approach used in this study is presented in the next section.

2.3. Precipitation in the interdiffusion zone

In principle, the PSD for precipitation in convective micromixers can be calculated by solving the population balance coupled with the continuity equation and the Navier–Stokes equation. However, the diffusion-precipitation process requires spatial resolutions below 1 μm whereas the global dimension of the mixing device is in the range of 1 mm, resulting in $O(1000^3)$ grid points. Since discretization of Eq. (5) with respect to L results in an additional hundred variables per grid point, $O(10^{11})$ equations would have to be solved for each time step.

Hence, a one-dimensional approach is applied in this study: while the population balance is implemented by direct simulation of Eq. (5), convective flow and global diffusion are modeled by means of lamellar stretching and the so-called interdiffusion zone. The convective eddies occurring in T-shaped micromixers roll up the initial two fluid lamellae thereby stretching them and reducing their lateral thickness, see Engler [20]. At the interface between the two fluid lamellae, barium chloride and sulfuric acid diffuse into each other, building up supersaturation. Thus precipitation starts at the interfacial area and propagates from there into the two lamellae. To estimate the width δ of this interdiffusion zone we use the characteristic length of diffusion:

$$\delta = \sqrt{2Dt} \tag{6}$$

With this notion we substitute the spatial varying values of nucleation rate $B(c(Ba^{2+}), c(SO_4{}^{2-}))$ and growth potential $\psi(c(Ba^{2+}), c(SO_4{}^{2-}))$ with their mean values $\langle B\rangle$ and $\langle\psi\rangle$ throughout the interdiffusion zone:

$$\begin{aligned}\langle\psi\rangle &= \frac{1}{\delta}\int_0^{\delta} \psi(c(Ba^{2+}), c(SO_4{}^{2-}))\,dx\\ \langle B\rangle &= \frac{1}{\delta}\int_0^{\delta} B(c(Ba^{2+}), c(SO_4{}^{2-}))\,dx\end{aligned} \tag{7}$$

Computation of these mean values requires estimates for the unknown concentration profiles of Ba^{2+} and $SO_4{}^{2-}$. The simplest model assumes a linear decrease of $c(Ba^{2+})$ and $c(SO_4{}^{2-})$ within the interdiffusion zone ($0 \le x \le \delta$) from bulk concentrations to zero.

Finally the effect of convective stretching has to be incorporated. This is accomplished by comparing the lamella width $w(t)$ with the interdiffusion width $\delta(t)$. The lamella contains the total solution volume $V_{sol} = w(t)A$ and the volume where nucleation occurs is given by $V_{nuc} = \delta(t)A$, with the interfacial area A. While $w(t)$ decreases with time, $\delta(t)$ increases continuously, and the nucleation volume ratio

$$\rho_{nuc} = \frac{V_{nuc}}{V_{sol}} = \frac{\delta(t)}{w(t)} \tag{8}$$

increases from 0 to 1. Thus, ρ_{nuc} is not only a measure for the mixedness, but also affects the population balance equation since n is the number of particles in the total solution volume whereas b is the number of particles formed in the nucleation volume. Hence, Eq. (5) must be modified appropriately:

$$\frac{\partial n}{\partial t} + \frac{\partial(Gn)}{\partial L} = \rho_{nuc} b \tag{9}$$

For T-shaped convective micromixers Engler [20] has proposed the *convective lamination model* with an exponentially decreasing lamella width:

$$w(t) = w_\infty + (w_0 - w_\infty)\exp\left(\frac{-t}{\tau_m}\right) \tag{10}$$

where w_0 is the initial lamella width. The final width w_∞ after decay of the convective eddies depends on kinematic viscosity υ, characteristic hydraulic diameter d_h, and the Re number:

$$w_\infty \approx \sqrt{\frac{8D}{\upsilon Re}}\,d_h. \tag{11}$$

The characteristic mixing time τ_m finally is estimated by

$$\tau_m \approx \frac{w_\infty}{2D}. \tag{12}$$

The details of the presented model are given in Kockmann et al. [21] along with the algorithm used for simulation. The results for precipitation of barium sulfate from 0.5 molar barium chloride solution and 0.33 molar sulfuric acid are displayed in the discussion along with the corresponding experimental results.

3. Fabrication and experimental investigation

To investigate different precipitation processes, silicon chips with a T-shaped mixing element and short mixing channel are designed and fabricated with DRIE etching, see Fig. 1, left side. The silicon chip is covered with a Pyrex glass lid to observe optically the nucleation and deposition process. To lower the risk of channel blockage the length of the mixing channel is reduced to the minimal value necessary for good mixing. Additionally the inlet and outlet connections are in the chip plane to avoid undesired bends and curves which facilitate an unwanted particle deposition. The chip has a footprint of 20 mm × 10 mm and a thickness of 1.025 mm. The nomenclature of the chip naming concerns the channel dimension of the symmetric T-shaped micromixers. The micromixer with the name T600 × 300 × 300 denotes a T-mixer with a mixing channel width of 600 μm, an inlet channel width of 300 μm, and an overall channel depth of 300 μm. The fabrication process of DRIE etching gives channels with uniform depth. If only the cross section of a channel is mentioned, the width and depth are given in μm. The T-shaped micromixers with short mixing channels are denoted with their length in 100 μm. For example, the mixer T-3-4 × 10 has an inlet channel width of 300 μm, a mixing channel width of 400 μm and length of 1000 μm. the overall channel depth is 300 μm, again.

3.1. Precipitation of barium sulfate

The mixing of sulfuric acid (0.33 mol/l, VWR) with barium chloride (0.5 mol/l, analytical grade, VWR) leads to the reactive

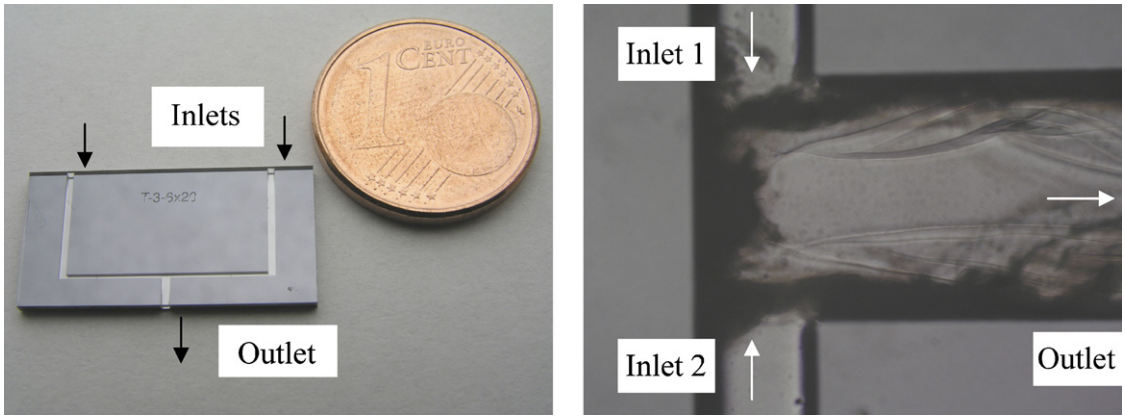

Fig. 1. Left: Silicon micromixer chip (10 mm × 20 mm footprint) designed for reactive precipitation. The short mixing channel with rectangular cross section (400 μm × 300 μm, 2 mm long) reduces the risk of blockage. Right: close-up of the T-junction during precipitation mixing of $BaSO_4$ (mixing ratio of 1:1). Particle laden streamlines show where the precipitation mainly occurs. The dark shaded areas are $BaSO_4$ depositions on the glass cover.

precipitation of barium sulphate according Eq. (1). The reactants are pumped by syringe pumps ("Injectomat 2000", Fresenius HemoCare) with an accurate adjustable flow rate up to 400 ml/h without flow pulsations. Due to the symmetric flow and mixing conditions, the *Re* number is taken in the mixing channel with the hydraulic diameter as the characteristic length.

The particle precipitation of $BaSO_4$ in the T-shaped micromixer is clearly visible in Fig. 1 right side. Some particles are deposited at the wall, visible as dark shadows. The nucleation in the flow is visible as curved streamlines. The streaks are indicating the engulfment flow regime and the mixing process within the T-shaped micromixer. After mixing, the suspension is collected in a beaker and analyzed with the laser light scattering instrument LS230 from CoulterBeckmann. The device measures particle diameters from 40 nm to 2000 μm.

In Fig. 2, left side, the number-based particle size distribution of $BaSO_4$ is shown for different *Re* numbers in the mixing channel. The mean particle diameter decreases for increasing *Re* numbers from 200 to 400, indicating the enhanced mixing process. With higher *Re* numbers, the mixing process deteriorates due to transient effects and vortex generation. This behavior is also observed with the iodide-iodate reaction in a T-shaped micromixer, see Fig. 2 right side. The segregation index of the parallel-competitive test reaction is a measure for the selectivity and the iodine concentration, and is inverse proportional to the mixing quality.

The entire PSD results for barium sulfate precipitation in T-shaped micromixers are presented in Table 1 for 0.33 molar sulfuric acid and 0.5 molar barium chloride solution mixed with equal flow rates. The indicated *Re* numbers refer to the total flow rate through the mixing channel. The four mixer types T-3-4 × 10, T-3-4 × 30, T-3-6 × 10 and T-3-6 × 30 have been investigated for various *Re* numbers from 200 to 500.

Considering the measured PSDs given in Table 1, the following systematic similarities can be noticed in all four mixer types:

- The mean diameter $\bar{L}$ falls at first with increasing *Re* number until a minimum is reached somewhere between *Re* = 300 and *Re* = 500. From there on, the mean diameter increases again towards an upper limit at approximately 120 nm. The sole exception is the T-3-6 × 30, for which the mean diameter remains at 91 nm for *Re* = 500.
- The standard deviation, $\sigma(L)$, decreases continuously for all mixer types for increasing *Re* numbers.

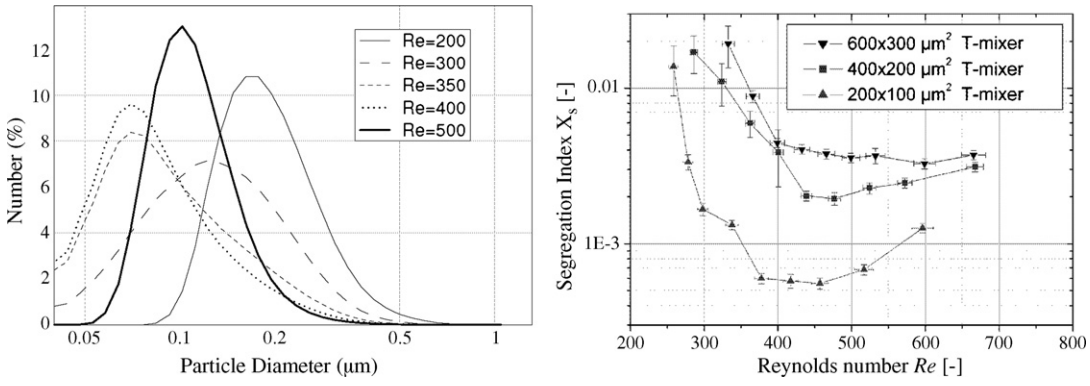

Fig. 2. Characterization of the mixing process in T-shaped micro mixers. Left: Comparison of particle size distributions PSD from reactive precipitation of $BaSO_4$ particles for different *Re* numbers in T-shaped micromixer (600 μm × 300 μm mixing channel area). Right: the segregation index from the Villermaux-Dushman iodide-iodate reaction is inversely proportional to the mixing quality, see also [14].

Table 1
Comparison of number-averaged mean diameter and standard deviation for barium sulfate precipitation by 1:1 mixing of 0.33 molar sulfuric acid and 0.5 molar barium chloride solution in four different T-shaped mixers (T-3-4 × 10, T-3-4 × 30, T-3-6 × 10, and T-3-6 × 30)

Re	$\bar{L}$ (nm)				σ_L(nm)			
	4 × 10	4 × 30	6 × 10	6 × 30	4 × 10	4 × 30	6 × 10	6 × 30
200	252.0	199.5	213.6	211.0	105.6	104.3	86.6	89.3
300	118.9	120.6	149.1	126.3	68.5	69.5	77.4	71.7
400	92.6	122.3	98.4	92.3	45.3	41.4	54.1	45.1
500	123.2	123.0	121.5	91.2	43.4	41.8	42.5	44.1
600	120.6	118.9	–	–	34.5	33.8	–	–

- A comparison of the different mixer types shows no systematic pattern in particle size and distribution for the same *Re* numbers.
- For low *Re* numbers, all mixers exhibit a secondary peak between 1 and 2 μm in the volume PSD. This peak diminishes with growing *Re* numbers.
- For medium *Re* numbers (between $Re = 300$ and $Re = 400$), the number percentages show a non-zero axis intercept. Hence, a considerable amount of particles is of sizes below the measurement limit of 40 nm, indicating that the applied PSD measurement method is reliable only to a certain degree.
- All PSDs are notedly skewed, i.e. they ascend rapidly from small sizes and decline gradually toward larger sizes. It is not clear, whether this effect is due to particle growth governed by mixing, particle aggregation, or the result of both phenomena.

An interesting relation between PSD and *Re* number can be depicted in a quite descriptive way if the peak in the number PSD is considered: it moves clockwise, starting at 3.00 h for $Re = 200$ and moving along with increasing *Re* number, until finally 12.00 h is reached. This movement is indicated by the dashed arrow in Fig. 2, left hand side. This development of the PSD with the *Re* number is a hint for the mixing quality development and will be part of further investigations.

Both, mean size and standard deviation tend toward lower values with increasing *Re* number, indicating an enhancement of mixing with formation of engulfment flow for $Re > 300$. At high *Re* numbers, the mean size seems to tend toward a limit value (≈100 nm), while the standard deviation keeps falling. Yet, the measured values are scattered over a comparatively broad range. The reason for this behavior is not clear, but unstable flow conditions due to the accelerated flow are one reasonable explanation. The decline of both characteristics with increasing *Re* numbers is more distinctive and the limit for $\bar{L}$ seems to be below the corresponding value for the T-3-4 mixers. No influence of the mixing channel length is observed.

3.2. Azo coupling and precipitation

Besides the $BaSO_4$ test reaction, the coupling step of azo compound pigments (i.e. dye particles) in convective micromixers is investigated with the pigment CLA1433 from Ciba. These experiments should investigate whether convective micromixers are appropriate for particle-laden/particle-generating flow under typical industrial conditions, and whether effectively operated micromixers can overcome drawbacks of conventional processes for azo pigment coupling. The basic idea is to enhance conversion with convective micromixers due to their rapid mixing process. The diazonium compound solution is prepared according to the process regulations for batch operation, only with dilution by a factor of 10 with water to reduce the particle concentration in the product flow. The diazonium solution and the solved coupling compound are mixed within a T-shaped convective mixer. The yielded product suspension is separated and analyzed with high-performance liquid chromatography (HPLC) by the analytical department at Ciba and compared to their reference standard for this product. All pigment samples contain a residual of precipitated coupling compound of more than 30 area percent (in the HPLC chromatogram) in the worst case, but only 6.5% in the best case. In comparison, the batch process reaches approximately 2–3 area percent of non-reacted coupling compound remaining in the batch product.

For the coupling experiments, three T-shaped micromixers were used with symmetric inlet flow conditions and a mixing channel with rectangular cross section (300 μm deep and 600 μm wide). The mixing channel length was 1, 2, and 3 mm, respectively. The net flow rate was varied to achieve *Re* numbers in the range between 500 and 1100. Blocking of the mixers occurred frequently after 2–3 min of operation, and predominantly at low flow rates and in mixers with a long outlet channel. Experiments with high flow rates (pump limit) could be finished without blocking which suggests that the blocking is not caused by gradual fouling, but rather by flow instabilities within the T-junction or flow pulsation into the opposite inlet channel. Additionally, high shear rates at high *Re* numbers do not allow the nanoparticle to attach and adhere at the channel walls. Flow pulsations at high *Re* numbers also hinder particles to adhere at the channel walls.

4. Discussion

Up to a *Re* number of 400 the mean particle diameter decreases. For higher *Re* numbers, the mean diameter increases, but the spread of the size distribution is noticeably reduced due to a change in the fluid dynamic mixing process. This corresponds with the mixing behavior in T-shaped micromixers, where the mixing quality increases with increasing *Re* number

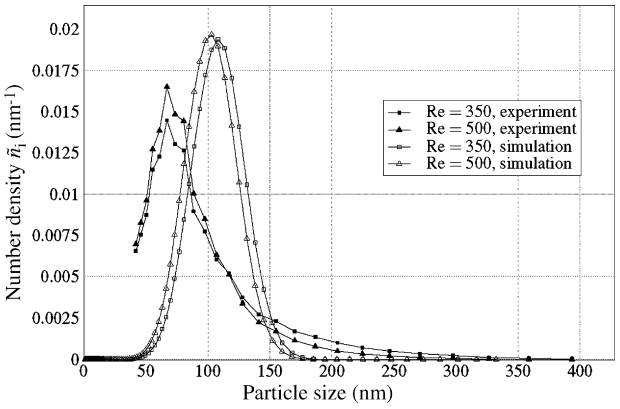

Fig. 3. Comparison of experimental $BaSO_4$ precipitation with numerical simulations of the PSD in a T-shaped micromixer with rectangular mixing channel cross section (600 μm wide and 300 μm deep). The uncertainty of experimental data is about 5% of the measured value.

first and decreases by transient vortex generation at approximately $Re = 300–500$.

Over a wide range of *Re* numbers, the experimental results show the same tendency as numerical simulation results using a simple convective mixing model with a population balance model. In Fig. 3, the typical PSD for two different *Re* numbers in the mixing channel of a T600 × 300 × 300 micromixer are displayed. With this background particle precipitation is also suitable to characterize the mixing process. Besides avoiding particle deposition in bends or curves, the main design rule for microstructured precipitation devices is to create a large interfacial area between the two fluid components. This is accomplished in convective micromixers like the T-mixer with *Re* numbers from 200 to 500 in the mixing channel. Particle attachment at the wall has to be avoided, mainly with straight channels without bends and curves. The inlet and mixing channel are located in one single layer (in-plane orientation) on the silicon chip. The silicone sealing enclosing the chip has straight connecting holes to avoid particle attachment especially for the mixing channel. The mixing channel is relatively short with 1–3 mm to minimize surface area in contact with particulate flow. This length is sufficiently long to allow almost complete mixing of the components. Further measures to avoid particle attachment at the wall are a sheath flow of clean fluid along the wall and special surface treatment. But this is not realized within this work.

For our devices, a feasibility study under industrial conditions has already demonstrated that microchannels are appropriate for precipitation processes. Summarizing for the industrial experiments, it can be stated that convective micromixers with short outlet channels are in principle suitable for the handling of particle-laden flow, although a mixer optimization with respect to backmixing and liability to flow pulsations is required. The desired full conversion to pigment CLA1433 was not accomplished. However, the production process for this pigment neither comes up to this goal and the batch process takes nearly a day and requires additives to reach 97% conversion, whereas the continuous micromixer process has a characteristic time of some milliseconds and uses no additives. The experiments were not operated under ideal conditions regarding the chemical conditions of the diazo coupling reactions. In particular, the optimization of pH with respect to the reaction rate of coupling should increase the yield for continuous processing.

5. Conclusion

This work presents theoretical and experimental investigations of precipitation processes. The developed convection-precipitation model couples the basic diffusive transport and thermodynamic precipitation theory with a convective mixing model for the T-shaped micromixer. A comparison with experimental results from $BaSO_4$ precipitation shows that this model can be used for a fast simulation of the particle size distribution for $Re > 350$. The model exhibits a rather good accordance with experimental particle size distributions regarding the mean particle size. For the higher distribution moments, e.g. the variance, the deviation is more evident and can be explained by model simplifications. The experimental results for $BaSO_4$ precipitation indicate the principle suitability of convective micromixers for nanoparticle generation. Instantaneous blocking, as encountered during pigment synthesis, is no issue with tiny particles in the range of approximately 100 nm. Yet, gradual fouling, like observed on the glass lid of the micromixers during the $BaSO_4$ experiments, can be problematic for long-term operation. The pigment synthesis results show that well-designed micromixers can even cope with highly particle-laden flows, if the device is tailored to the operation conditions. Thus, an appropriate design and a careful selection of the employed materials and surfaces, or simply the use of disposable mixers can overcome drawbacks that currently hinder the application of micromixers in reactive precipitation.

Acknowledgements

The experimental part of this work was partly supported by Ciba Specialty Chemicals Inc. (Ciba), which we gratefully acknowledge. The particle size measurements were performed in collaboration with the Laboratory for Materials Process Technology, IMTEK, University of Freiburg.

References

[1] N. Kockmann, Transport processes and exchange equipment, in: N. Kockmann (Ed.), Micro Process Engineering, Wiley-VCH, 2006, pp. 71–113, Chapter 3.
[2] H.-C. Schwarzer, Nanoparticle precipitation—an experimental and numerical investigation including mixing, Dissertation, University Erlangen-Nürnberg, Logos Verlag, Berlin, 2005.
[3] H.-C. Schwarzer, W. Peukert, Experimental investigation into the influence of mixing on nanoparticle precipitation, Chem. Eng. Technol. 25 (2002) 657–661.
[4] H.-C. Schwarzer, W. Peukert, Combined experimental/numerical study on the precipitation of nanoparticles, AIChE J. 50 (2004) 3234–3247.
[5] H.-C. Schwarzer, F. Schwertfirm, M. Manhart, H.-J. Schmid, W. Peukert, Predictive simulation of nanoparticle precipitation based on the population balance equation, Chem. Eng. Sci. 61 (2006) 167–181.

[6] Y.-J. Choi, S.-T. Chung, M. Oh, H.-S. Kim, Investigation of crystallization in a jet y-mixer by a hybrid computational fluid dynamics and process simulation approach, Cryst. Growth Design 5 (2005) 959–968.
[7] M. Schur, B. Bems, A. Dassenoy, I. Kassatkine, J. Urban, H. Wilmes, O. Hinrichsen, M. Muhler, R. Schlögl, Kontinuierliche Cofällung von Katalysatoren in einem Mikromischer: nanostrukturierte Cu/ZnO-Komposite für die Methanolsynthese, Angew. Chem. 115 (2003) 3945–3947.
[8] V.S. Shirure, A.S. Pore, V.G. Pangarkar, Intensification of precipitation using narrow channel reactors: magnesium hydroxide precipitation, Ind. Eng. Chem. Res. 44 (2005) 5500–5507.
[9] H. Pennemann, S. Forster, J. Kinkel, V. Hessel, H. Löwe, L. Wu, Improvement of dye properties of the azo pigment yellow 12 using a micromixer-based process, Org. Proc. Res. Dev. 9 (2005) 188–192.
[10] Clariant International LTD, Verfahren zur Herstellung von Diketopyrrolopyrrol-Pigmenten, European patent application, EP 1,162,240 A2.
[11] Clariant International LTD, Verfahren zur Konditionierung von organischen Pigmenten, European patent application, EP 1,167,461 A2.
[12] V. Hessel, H. Löwe, A. Müller, G. Kolb, Chemical Micro Process Engineering, Chap. 1. Mixing of miscible fluids, Wiley-VCH, 2005, pp. 1–280.
[13] N. Kockmann, T. Kiefer, M. Engler, P. Woias, Convective mixing and chemical reactions in microchannels with high flow rates, Sens. Actutors, B B117 (2006) 495–508.
[14] N. Kockmann, T. Kiefer, M. Engler, P. Woias, Silicon microstructures for high throughput mixing devices, Microfluid. Nanofluid. 2 (2006) 327–335.
[15] N. Kockmann, S. Dreher, P. Woias, Unsteady Laminar Flow Regimes and Mixing in T-Shaped Micromixers, ASME-ICNMM2007-30041, 2007.
[16] C. Monnin, A thermodynamic model for the solubility of barite and celestite in electrolyte solutions and natural seawater to 200 °C and 1 kbar, Chem. Geol. 153 (1999) 187–209.
[17] O. Söhnel, J. Garside, Precipitation: Basic Principles and Industrial Applications, Butterworth-Heinemann, Oxford, 1992.
[18] A. Mersmann, K. Bartosch, B. Braun, A. Eble, C. Heyer, Möglichkeiten einer vorhersagenden Abschätzung der Kristallisationskinetik, Chem. Ing. Tech. 72 (2002) 17–30.
[19] A.D. Randolph, M.A. Larson, Theory of Particulate Processes, Academic Press, London, 1988.
[20] M. Engler, Simulation, Design, and Analytical Modelling of Passive Convective Micromixers for Chemical Production Purposes, Shaker, Aachen, 2006.
[21] N. Kockmann, J. Kastner, P. Woias, Numerical and experimental study of nanoparticle precipitation in microreactors, Il Ciocco, Barga, 11–15, June, in: ESI 2nd Int. Conf. Transport Phenomena Micro Nanodevices, 2006.